

## Time-dependent reliability analysis of flood defenses under cumulative internal erosion

Pol, Joost; Kanning, Wim; Jonkman, Sebastiaan N.; Kok, Matthijs

**DOI**

[10.1080/15732479.2024.2416434](https://doi.org/10.1080/15732479.2024.2416434)

**Publication date**

2024

**Document Version**

Final published version

**Published in**

Structure and Infrastructure Engineering

**Citation (APA)**

Pol, J., Kanning, W., Jonkman, S. N., & Kok, M. (2024). Time-dependent reliability analysis of flood defenses under cumulative internal erosion. *Structure and Infrastructure Engineering*. <https://doi.org/10.1080/15732479.2024.2416434>

**Important note**

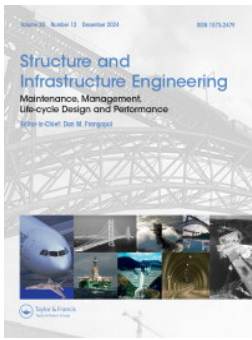
To cite this publication, please use the final published version (if applicable). Please check the document version above.

**Copyright**

Other than for strictly personal use, it is not permitted to download, forward or distribute the text or part of it, without the consent of the author(s) and/or copyright holder(s), unless the work is under an open content license such as Creative Commons.

**Takedown policy**

Please contact us and provide details if you believe this document breaches copyrights. We will remove access to the work immediately and investigate your claim.



# Structure and Infrastructure Engineering

## Maintenance, Management, Life-Cycle Design and Performance

ISSN: (Print) (Online) Journal homepage: [www.tandfonline.com/journals/nsie20](http://www.tandfonline.com/journals/nsie20)

## Time-dependent reliability analysis of flood defenses under cumulative internal erosion

Joost Pol, Wim Kanning, Sebastiaan N. Jonkman & Matthijs Kok

To cite this article: Joost Pol, Wim Kanning, Sebastiaan N. Jonkman & Matthijs Kok (24 Oct 2024): Time-dependent reliability analysis of flood defenses under cumulative internal erosion, Structure and Infrastructure Engineering, DOI: [10.1080/15732479.2024.2416434](https://doi.org/10.1080/15732479.2024.2416434)

To link to this article: <https://doi.org/10.1080/15732479.2024.2416434>



© 2024 The Author(s). Published by Informa UK Limited, trading as Taylor & Francis Group



Published online: 24 Oct 2024.



Submit your article to this journal [↗](#)



Article views: 93



View related articles [↗](#)



View Crossmark data [↗](#)

# Time-dependent reliability analysis of flood defenses under cumulative internal erosion

Joost Pol<sup>a,b</sup>, Wim Kanning<sup>a,c</sup>, Sebastiaan N. Jonkman<sup>a</sup> and Matthijs Kok<sup>a,b</sup>

<sup>a</sup>Hydraulic Engineering, Delft University of Technology, Delft, Netherlands; <sup>b</sup>HKV, Lelystad, Netherlands; <sup>c</sup>Deltares, Delft, Netherlands

## ABSTRACT

Internal erosion is a significant cause of failure in dams, levees and other hydraulic structures. This article studies the time-dependent reliability of such structures under Backward Erosion Piping (BEP), a form of internal erosion in the foundation. First, a physics-based time-dependent piping failure model is presented. Second, a time-variant reliability analysis method is presented which allows to quantify how the reliability evolves over the years due to cumulative pipe growth over multiple flood events. Finally, these models are used to study the importance of time-dependence for reliability estimates of flood defenses in The Netherlands. The findings show that, particularly in coastal areas, incorporating time-dependence significantly reduces the computed failure probability. Reductions vary widely, ranging from a factor of 5 to more than  $10^6$ , depending on flood duration and levee properties. Therefore, reliability estimates for levees can be improved by incorporating time-dependent pipe development in the BEP failure model, and thereby contribute to avoiding unnecessary reinforcements.

## ARTICLE HISTORY

Received 1 February 2024  
Revised 7 June 2024  
Accepted 26 August 2024

## KEYWORDS



Backward erosion piping; flood defense structures; flood risk; internal erosion; levees; load duration; reliability; time-variant

## 1. Introduction

Structural flood protection measures such as levees and dams play an important role in flood risk reduction strategies (Jonkman, 2005; Wesselink et al., 2016). Proper flood risk assessments and effective risk-based decision-making require accurate estimates of the reliability or failure probability of such flood defenses. Failures of dams and levees are frequently attributed to internal erosion or backward erosion piping (Danka & Zhang, 2015; Foster, Fell, & Spannagle, 2000; Özer, van Damme, & Jonkman, 2019). Consequently, understanding and quantifying the probability of this failure mechanism is important for determining the overall reliability of flood defenses. However, loads and strength of flood defenses may change over time, posing challenges on the quantification of the structure's reliability (Jonkman, Voortman, Klerk, & van Vuren, 2018). This paper quantifies backward erosion piping reliability from a time-dependent perspective. This is especially relevant for hydraulic structures where the hydraulic load has a time-scale shorter than that of the erosion process from initiation to catastrophic failure. Besides yielding more accurate reliability estimates, insights in the time scale of failure can inform emergency response decisions when piping is observed.

Backward erosion piping (BEP) is a geotechnical failure mechanism by which groundwater flow beneath a hydraulic structure erodes the granular foundation, which is covered by a cohesive blanket layer (Figure 1). This is observed both

at rigid structures such as weirs (Bligh, 1910) and soil structures such as levees or dams (Foster et al., 2000). Piping occurs as a series of sequential processes. High water levels resulting from extreme events (storm surge, river flood) induce high pore pressures in the aquifer. Excess pressures at the downstream levee toe can lead to uplift and rupture of a cohesive blanket, creating an unfiltered exit point in the form of a crack. Subsequently, sand is transported vertically through the crack. The transported sand creates a void (called pipe) which develops in backward direction toward river. When the pipe reaches the river, flow intensifies, and the pipe's cross-section enlarges (also called widening). Ultimately, this leads to instability and collapse of the levee, either by gradual settlement or instability of the embankment. The erosion process ceases upon successful application of flood fighting interventions (e.g. sandbags to reduce hydraulic head) or when the water level decreases sufficiently. Further details on the mechanisms can be found in van Beek (2015), ICOLD (2017) and Rice, van Beek, and Bezuijen (2021). Most research on BEP focused primarily on the critical load at which BEP leads to failure (van Beek, 2015). However, recent investigations have also studied time-dependent aspects of the erosion process, either experimentally (Allan, 2018; Pol, Kanning, van Beek, Robbins, & Jonkman, 2022; Riha & Petrula, 2023; Robbins, van Beek, López-Soto, Montalvo-Bartolomei, & Murphy, 2018; Vandenboer, Celette, & Bezuijen, 2019) or using numerical modeling (Rotunno, Callari, & Froiio, 2019; Wewer, Aguilar-López, Kok, & Bogaard, 2021).

CONTACT Joost Pol  pol@hkv.nl  Delft University of Technology, Stevinweg 1, 2628 CN Delft, Netherlands.

© 2024 The Author(s). Published by Informa UK Limited, trading as Taylor & Francis Group  
This is an Open Access article distributed under the terms of the Creative Commons Attribution License (<http://creativecommons.org/licenses/by/4.0/>), which permits unrestricted use, distribution, and reproduction in any medium, provided the original work is properly cited. The terms on which this article has been published allow the posting of the Accepted Manuscript in a repository by the author(s) or with their consent.

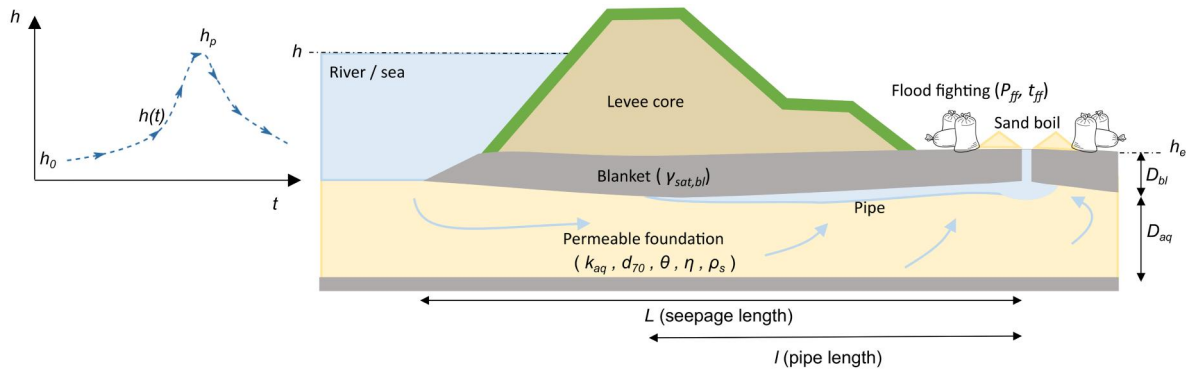


Figure 1. Illustration of backward erosion piping in a levee on a sandy foundation and definition of variables used in the analysis.

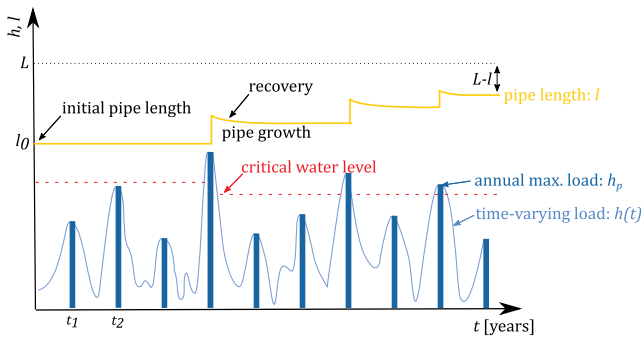


Figure 2. Illustration of time-dependent pipe length development over a 10-year period.

Effects of time-dependency are present in most parts of the failure process, mainly being (1) the duration of the hydraulic load, (2) the response of aquifer pore pressures to this load and associated effects on blanket uplift, and (3) backward pipe growth. Most prediction models used in practice assume a constant water level, steady-state groundwater flow, and instantaneous pipe progression once a critical condition is exceeded. This article focuses on the relation between the first and third factor: if the pipe grows relatively slowly compared to the flood duration, water levels may recede before the pipe has fully developed into a failure. Analysis of historical levee failure cases due to BEP in different countries indicates that the time required for the failure to develop can be significant in some cases (Pol, 2022). In addition to this time-dependence within an extreme event, it also appears in a long-term evolution of the reliability over multiple years. When pipes develop only partially during an event, this creates a different initial condition for the next high water event. The presence of a partially developed pipe before a new flood occurs, implies that less time is needed for the pipe to progress through the foundation. Consequently, the resistance against piping may decrease over the years (Figure 2). Although this may be compensated by strength recovery in the period between flood events, current knowledge is insufficient to quantify the degree and rate of recovery.

Structural reliability analysis is a process to determine the safety level of a structure or system (e.g. Baecher & Christian, 2005; Melchers & Beck, 2017). In the context of flood defenses, this is interpreted as the probability of flooding of a protected area. This requires the definition of a

failure model and limit state function (LSF), statistical distributions for model inputs such as levee properties, and a suitable probabilistic computational method. Examples of time-invariant BEP reliability analyses are Calle et al. (1985), Vrijling (2001), Wolff (2008), and Rice and Polanco (2012). Calle et al. (1985) already recommended to include the time scale of BEP in reliability analyses, but this aspect has received little attention so far. Three reliability studies that represent BEP as a time-dependent process (Buijs, Hall, Sayers, & Van Gelder, 2009; Chen & Mehrabani, 2019; Vorogushyn, Merz, & Apel, 2009) are discussed in Section 2.1, including proposed improvements in the analysis method based on recent insights about the BEP process.

This article aims to quantify to which extent time-dependent development of piping affects the time-variant reliability of levees compared to an analysis in which piping is considered as instantaneous failure process. Therefore, a new piping failure model is developed which describes the relevant processes (uplift, heave, backward erosion, flood fighting) in an integrated manner, and this model is integrated in a time-variant reliability method. The analyses focus on the contribution of time-dependent erosion to the reliability, and how this depends on the characteristics of hydraulic loads, levee and subsoil properties and flood fighting operations. This article is partly based on a doctoral dissertation (Pol, 2022).

## 2. Method

After discussing previous studies (Section 2.1), this section describes the methods used in this article to analyze the time-variant reliability of levees with respect to the failure mechanism backward erosion piping. This includes both the pipe progression model (Section 2.3) and the probabilistic methods (Section 2.4).

### 2.1. Previous studies on time-variant piping reliability

Three studies that describe a reliability method in which BEP is represented as a time-dependent process are discussed below and summarized in Table 1. Buijs et al. (2009) developed a method for analyzing time-dependent flood defense reliability over the lifetime of the structure, including an example for piping. The evolution of degrading

Table 1. Summary of time-dependent BEP analyses in previous studies.

Aspect	Buijs et al. (2009)	Vorogushyn et al. (2009)	Chen and Mehrabani (2019)
Time-variant reliability	Yes: stochastic process and hierarchical process	No	Yes: semi-Markov process
Limit state definition	Critical water level based on Sellmeijer (1988)	Hydraulic shortcut due to BEP: pipe length equals seepage length.	Critical water level based on Weijers and Sellmeijer (1993)
Deterioration mechanism	Seepage length reduction	Pipe length development	Seepage length reduction
Deterioration rate	Hierarchical process: rate is a function of permeability and acting hydraulic gradient.	Deterministic pipe progression rate based on a large-scale experiment	Distribution depending on condition grade (estimated by expert judgment)

parameters is modeled using stochastic (Gamma) processes and a physics-based (hierarchical) process model in which the seepage length decreases depending on the applied water level. This physics-based model is equivalent to that of Kézdi (1979), with the exception of porosity being excluded. Subsequently, the degrading seepage length is used in the Sellmeijer (1988) model to obtain a degrading critical head. Modeling long-term degradation of piping resistance using stochastic processes has disadvantages. Most important, parameters of the stochastic process are hard to determine for practical applications because pipe length development is hard to observe. Therefore, a physics-based model for pipe length development is needed. Additionally, pipe growth is likely not independent from year to year, as it depends on uncertain but constant levee properties and may accelerate over time, depending on the physical model used.

Vorogushyn et al. (2009) developed levee fragility curves for piping and micro-instability, which describe the failure probability conditional on the hydraulic load (peak and duration). The study is limited to failure within a single extreme event and does not analyze long-term reliability under multiple events. In their physics-based analysis, piping failure is considered a combination of four processes: (1) transient seepage, (2) blanket uplift, (3) exceedance of a critical head for BEP, ultimately leading to (4) the formation of a hydraulic shortcut due to BEP. Although at that time, hardly any information on the rate of pipe growth was available, they included this process in the analysis by assuming a deterministic progression rate of 0.158 m/hour ( $4.4 \cdot 10^{-5}$  m/s) based on a single large-scale experiment (Weijers & Sellmeijer, 1993). The authors recommend further research to quantify this progression rate (including the effects of sand properties and hydraulic loading), as it was found to have a significant impact on the computed failure probability.

Chen and Mehrabani (2019) developed a method for the time-dependent reliability of coastal flood defenses and included piping degradation over time by reducing the seepage length according to Weijers and Sellmeijer (1993). They applied a semi-Markov deterioration modeling approach, where the levee is represented by discrete states (condition grades), and the transition probability from the current condition grade to a degraded condition grade depends on the time that the levee has been in the current state. The reduction of the seepage length in Sellmeijer's prediction model for the critical head is similar to Buijs et al. (2009). The difference is that Chen and Mehrabani (2019) assume specific degrees of seepage length reduction based on the levee's condition grade, which can be determined using expert

judgment or inspections. As a result, the method is less suitable for a more physics-based description of pipe length development as a function of hydraulic loads and subsoil characteristics.

To summarize, Buijs et al. (2009) and Chen and Mehrabani (2019) focused on the long-term development (lifetime), while Vorogushyn et al. (2009) only included pipe development during a single extreme event. However, the description of pipe development in Vorogushyn et al. (2009) has a stronger physical basis. Given recent insights into the time-dependent development of BEP from experimental and modeling perspectives (Pol, 2022), there are potential improvements that can be made to the methods used in the above-mentioned studies:

- Define failure as a pipe progressing entirely through the levee foundation, instead of the head exceeding the critical head.
- Include a time-varying water level within a storm event, instead of a block shape as used in Buijs et al. (2009) and Chen and Mehrabani (2019).
- Allow the progression rate to vary over time within a storm event as function of water level and levee properties, with this function being validated on physical experiments and numerical modeling.
- Include a threshold below which no erosion occurs as the grains in the pipe are in equilibrium, for instance the equilibrium head  $H_{eq}(l)$ .
- Include blanket uplift, flow resistance in the vertical crack, and flood fighting interventions, including their timing within an event, as factors that limit the time available for pipe growth.

## 2.2. General piping reliability formulation

Levee reliability is defined as the probability that a levee fulfills its function (i.e. does not fail) during a given period of time. Failure is governed by a combination of variables, which can be described using time-invariant random variables and time-variant ones (stochastic processes). For levees, piping failure is caused by extremely high water levels (hydraulic loads) from storm surges or river floods, which lead to strength degradation by increasing the eroded pipe length once a critical water level is exceeded (Figure 2). In general, a time-dependent reliability problem can be formulated as (e.g. Melchers & Beck, 2017):

$$P_f(t) = P(g(\mathbf{X}(t)) \leq 0) = \int_{g(\mathbf{X}(t)) \leq 0} f_{\mathbf{X}(t)}(\mathbf{x}(t)) \cdot d\mathbf{x}(t) \quad (1)$$

where  $P_f$  denotes the probability of being in the failed state in year  $t$ ,  $\mathbf{X}$  is a vector of random variables,  $g(\cdot)$  the limit state function and  $f_{\mathbf{X}(t)}(\mathbf{x}(t))$  the joint probability density of the random variables. Classical approaches to solve this reliability problem are sampling based methods such as Monte Carlo Simulation (MCS) (Rubinstein & Kroese, 2008) and approximation methods such as the first-order reliability method (FORM) (Hasofer & Lind, 1974).

The probability in Equation (1) is interpreted as a cumulative or lifetime failure probability: the probability that failure occurs between the start of the analysis and year  $t$ . The probability that failure occurs exactly in year  $t$  is given by  $dP_f(t)/dt$ . The conditional failure rate  $\lambda(t)$  (also called hazard function) is the probability that failure occurs in year  $t$  given that no failure occurred in the years before year  $t$ . It can be computed from Equation (1) by JCSS (2001):

$$\lambda(t) = \frac{dP_f(t)/dt}{1 - P_f(t)} \quad (2)$$

Piping failure occurs when a pipe has progressed through the levee foundation creating a hydraulic shortcut. Therefore, the limit state function (LSF) for BEP is defined as the difference between seepage length  $L$  and pipe length  $l$  (Vorogushyn et al., 2009). In the time-variant analysis, the pipe length at the end of a flood event  $l_e$  is used:

$$g(\mathbf{X}) = L - l_e \quad (3)$$

and Equation (1) can be rewritten as:

$$P_f(t) = P(l_e(t) \geq L) \quad (4)$$

Although this LSF seems very simple,  $l_e(t)$  is a function of many variables such as the initial pipe length, extreme hydraulic loads (peak level & duration), time-invariant levee properties, and flood fighting interventions. The function is given by the pipe progression model as described in Section 2.3. Furthermore, these underlying variables have different statistical characteristics with respect to correlation between years, which is discussed in Section 2.4.1.

### 2.3. Pipe progression model

The pipe progression model in this section describes the time-dependent development of pipe length  $l(t)$  under a given hydraulic load event and contains both physical processes (blanket uplift, pipe erosion) and human actions (flood fighting). Equation (5) gives the instantaneous progression rate [m/s], which is based on a curve-fit on simulations with a finite element model which was calibrated and validated on multi-scale piping experiments (Pol, Noordam, & Kanning, 2024). The pipe only progresses if a set of conditions ( $I_{er}$ ) is satisfied, as specified in Equation (7)

$$\frac{dl}{dt} = \begin{cases} 89 \cdot C_e \left( k \frac{H(t) - H_{eq}(t)}{L} \right)^{0.81} & \text{if } I_{er} = \text{true} \\ 0 & \text{else} \end{cases} \quad (5)$$

$C_e$  denotes an erosion coefficient [–],  $k$  hydraulic conductivity [m/s],  $H$  imposed head difference [m],  $H_{eq}$  equilibrium head [m],  $L$  seepage length [m], 89 and 0.81 are regression

coefficients (Pol et al., 2024). Here,  $t$  describes the time within a flood event, hence a much shorter time scale than the time-dependent reliability problem in Section 2.4 where  $t$  is expressed in years. The imposed head difference is reduced by a head loss over the blanket (vertical pipe) due to resistance of the fluidized sediment (e.g. Schweckendiek, Vrouwenfelder, & Calle, 2014; TAW, 1999):

$$H = h - h_e - 0.3D_{bl} \quad (6)$$

where  $h$  is outer water level,  $h_e$  polder level at the exit point and  $D_{bl}$  polder blanket thickness.

The required conditions for pipe progression: (1) blanket uplift has occurred previously, either in the current event or in past events; (2) heave (vertical transport through the crack) is possible at the current time step; (3) flood fighting interventions have not been taken (yet) at the current time step. These conditions are expressed in  $I_{er}$  as:

$$I_{er}(t) = \left( \min_{0 \dots t} \{Z_u(t)\} < 0 \cup l_{ini} > 0 \right) \cap (Z_h(t) < 0) \cap (t < t_{uh} + (t_{ff}/I_{ff})) \quad (7)$$

where  $l_{ini}$  is the initial pipe length at the start of the flood event,  $t_{uh}$  is the first time that uplift and heave and erosion ( $H > H_{eq}$ ) occur within the flood event (proxy for sand boil formation),  $t_{ff}$  is the time required for successful flood fighting and  $I_{ff}$  is an indicator which is 1 in case of successful flood fighting and 0 otherwise. The limit states for uplift ( $Z_u$ ) and heave ( $Z_h$ ) are given by (e.g. Schweckendiek et al., 2014; TAW, 1999):

$$Z_u(t) = (\varphi_{it}(t) - h_e) - D_{bl} \cdot (\gamma_{bl,sat} - \gamma_w) / \gamma_w \quad (8)$$

$$Z_h(t) = (\varphi_{it}(t) - h_e) / D_{bl} - i_{c,h} \quad (9)$$

$$\varphi_{it}(t) = h_e + r_e \cdot (h(t) - h_e) \quad (10)$$

where  $\varphi_{it}$  [m] denotes the aquifer head at the inner levee toe,  $r_e$  the head response factor to an increase in water level,  $\gamma_{bl,sat}$  the saturated blanket weight [kN/m<sup>3</sup>],  $\gamma_w$  the water weight [kN/m<sup>3</sup>] and  $i_{c,h}$  the critical heave gradient [–].

Flood fighting interventions are included in the model in two ways: by the probability of a successful detection (through  $I_{ff}$ ) and by the time required for successful flood fighting ( $t_{ff}$ ), see Equation (7). In case the initiation of piping (a sand boil) is not detected,  $I_{ff} = 0$  and the term  $t_{ff}/I_{ff}$  becomes  $\infty$ . The time required for successful flood fighting is a lumped parameter representing all actions since the moment of sand boil formation (initiation), and includes required time for detection of the sand boil, mobilization of staff and materials, and placement of the intervention. Equation (7) assumes binary intervention effects: either successful (i.e. completely stops pipe growth) or unsuccessful.

The progression rate depends on constant levee properties (e.g.  $C_e$ ,  $k$ ,  $d_{70}$ ,  $L$ ) and time-varying variables ( $H$ ,  $H_{eq}$  and  $l$ ). The equilibrium curve  $H_{eq}(l)$  is defined by linear interpolation between the following three points (Figure 3):

$$\begin{aligned} H_{eq}(0) &= 0 \\ H_{eq}(l_c) &= H_c \\ H_{eq}(L) &= 0.9H_c \end{aligned} \quad (11)$$

Here  $H_c$  and  $l_c$  are the critical head and critical pipe length for backward erosion, respectively. The linear

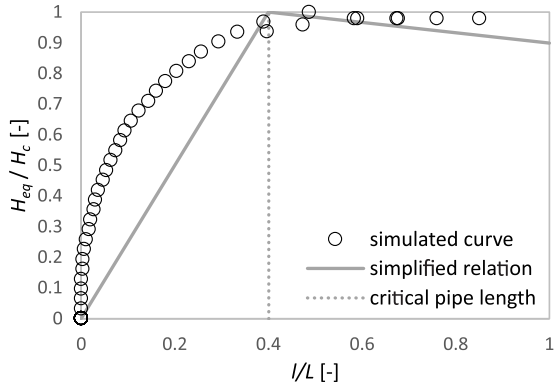


Figure 3. Equilibrium curve from numerical simulations and simplified relation used in pipe progression model.

interpolation to the points  $(0,0)$  and  $(L, 0.9H_c)$  is a conservative estimate based on equilibrium curves following from the numerical simulations in Pol et al. (2024).

The critical head  $H_c$  for backward erosion is based on the revised Sellmeijer model (Sellmeijer, de la Cruz, van Beek, & Knoeff, 2011):

$$H_c = L \cdot F_r \cdot F_s \cdot F_g$$

$$F_r = \eta \frac{\rho_s - \rho_w}{\rho_w} \tan \theta \left( \frac{D_r}{D_{r,m}} \right)^{0.35} \left( \frac{C_u}{C_{u,m}} \right)^{0.13} \left( \frac{KAS}{KAS_m} \right)^{-0.02}$$

$$F_s = \frac{d_{70}}{\sqrt[3]{\kappa L} \left( \frac{d_{70,m}}{d_{70}} \right)^{0.6}}, \kappa = k \frac{\nu}{g} F_g = 0.91 \left( \frac{D}{L} \right)^{0.28 / [(D/L)^{2.8} - 1] + 0.04}$$
(12)

Here  $\rho_s$  and  $\rho_w$  denote the sediment and water density [ $\text{kg}/\text{m}^3$ ],  $\eta$  the coefficient of White [–],  $\theta$  the angle of repose [deg],  $D_r$  the relative density [–],  $C_u$  the uniformity coefficient [–], KAS the angularity [–],  $d_{70}$  the grain size [m],  $\kappa$  intrinsic permeability [ $\text{m}^2$ ],  $k$  hydraulic conductivity [m/s],  $\nu$  kinematic viscosity of water ( $1.3 \cdot 10^{-6} \text{ m}^2/\text{s}$ ),  $L$  seepage length [m],  $D$  aquifer thickness [m].  $D_{r,m} = 0.725$ ,  $d_{70,m} = 2.08 \cdot 10^{-4} \text{ m}$ ,  $C_{u,m} = 1.81$  and  $KAS_m = 0.498$  are mean values in the experiments used for the multivariate regression. In this article, the effect of  $D_r$ ,  $C_u$  and KAS is neglected by choosing their values equal to the mean values.

A simple function is proposed for the critical pipe length of backward erosion  $l_c$  (Equation (13)). For homogeneous aquifers, this function agrees well with 2D numerical piping model simulations such as those from Sellmeijer (2006) and Rosenbrand et al. (2022).

$$\frac{l_c}{L} = \frac{1}{2} \cdot \tanh \left( 2 \frac{D}{L} \right)$$
(13)

Equations (5)–(13) provide the pipe growth model. Figure 4 shows a deterministic example of the pipe length development during a coastal storm surge. Pipe growth starts when both uplift and heave have occurred, and continues until a flood fighting intervention stops it after 10 h ( $t_{ff}$ ). In this case, no failure occurs because  $l/L \approx 0.1 < 1$  at the end of the storm event. In this example, the critical water level for BEP is approximately 5 m + NAP and a steady-state model would predict failure. Although this critical level is exceeded by one meter, the storm event is too

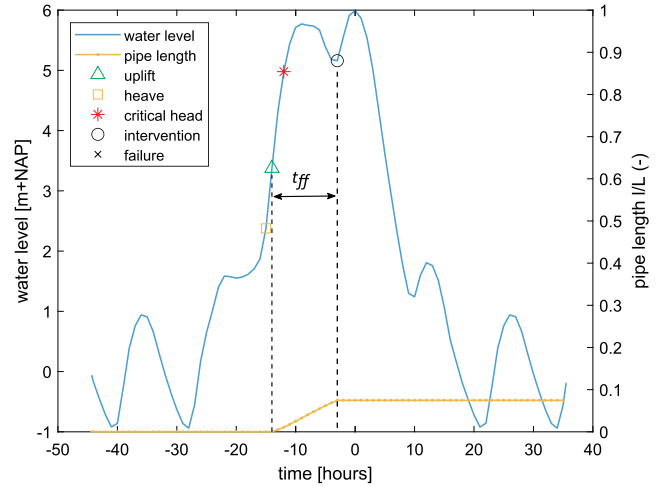


Figure 4. Example of pipe development for coastal levee. One realization of the base case as described in section 3.1 with  $D_p = 4 \text{ h}$ ,  $h_p = 6 \text{ m} + \text{NAP}$  and  $l_{mi} = 0$ .

short to result in failure and the flood fighting intervention is taken in time.

## 2.4. Probabilistic method

### 2.4.1. Character of piping uncertainties

The piping erosion process is driven by extreme high water levels, in combination with levee properties governing the levee resistance against these loads, and sometimes human actions such as flood fighting interventions. It is a deterioration process with a rate of deterioration given by the pipe progression rate, which depends on the hydraulic loads, strength properties and on previous pipe growth. The statistical characteristics of the random variables of loads and resistance that govern BEP have implications for the choice of probabilistic method.

Two main types of uncertainties are distinguished (Paté-Cornell, 1996; Slijkhuis, Van Gelder, Vrijling, & Vrouwenvelder, 1999): (1) aleatory or inherent uncertainty representing random variations in time (or space) and (2) epistemic uncertainty representing a lack of knowledge or data. The difference between those types is relevant for time-variant reliability because it affects the correlation between the structural performance over time (Kiureghian & Ditlevsen, 2009). For piping reliability, hydraulic loads such as annual maximum water levels can be considered aleatory uncertainty and independent between years (each year, this variable has a new value). Levee properties and model parameters are classified as epistemic and fully dependent between years (each year, this variable has the same but unknown value). Uncertainties in successful flood fighting may contain both types of uncertainty and are partly dependent between years. Due to this dependence over time, the structural performance  $g(\mathbf{X})$  in subsequent years is also correlated. As the pipe length depends on all other load and strength variables, it is affected by both types of uncertainty.

A suitable probabilistic method must be able to model these different types of dependencies in time and still be

efficient. Computational efficiency is important because levee safety standards require small failure probabilities, in the order of  $10^{-2}$  to  $10^{-6}$  per year for levee segments of 20–30 km length, and several orders of magnitude stricter requirements for individual cross sections. Furthermore, the two probabilistic methods described in this section allow for the following characteristics:

- levee properties and flood fighting effectiveness are considered constant over time but affect the pipe progression rate.
- extreme loads (yearly maximum water level, duration) occur independently from both the levee properties and the previous pipe growth. The maximum level and duration are uncorrelated.
- extreme loads are uncorrelated in time as long as a sufficiently large time interval is used (years).
- loads may change over time due to sea level rise or changing river discharges.

#### 2.4.2. Hydraulic loads

Before describing the two probabilistic methods, the modeling of hydraulic loads is discussed first, as it plays a role in each method. Essentially, the load (water level) is a stochastic process. In both methods, the variability in water level is simplified. Since the piping erosion process is driven by extreme water levels and the probability of multiple independent extreme events in a year is assumed to be negligible, only the yearly maximum event is considered. Therefore, the water level variability is simplified to an extreme value distribution of the yearly maximum water level  $h_p$ . Hence the time step  $\Delta t$  in the time-dependent reliability analysis is 1 year.

Variation of the water level over time within this annual maximum event is also simplified, depending on the origin of the extreme event (coastal storm surge or river flood), see Section 3.1.2 for more details. For the understanding of the probabilistic methods in this section, it is sufficient to note that the water level is described by two random variables: peak water level  $h_p$  and peak duration  $D_p$ . A more rigorous method would be to base the variability on a large set of hydrographs from ensemble simulations with a model with coupled weather and hydraulics, but this is beyond the scope of this article because of the high computational cost.

Because of the small failure probabilities and extreme value distributions of the hydraulic load (water level), the computation can be made more efficient by separating the hydraulic loads and levee properties. The following subsections describe two methods with different approaches to separate the hydraulic loads and levee properties. The first method (A) is a Crude Monte Carlo benchmark method, where no separation occurs. This method requires more computational time for small failure probabilities and therefore it is only used to validate method B. Method B applies Numerical Integration (NI) for the time-variant variables (peak water level, peak duration, and pipe length) to efficiently compute extreme events, and Monte Carlo

Simulation (MCS) for the time-invariant variables (uncertain levee properties). This approach allows for fewer model evaluations in the case of small probabilities.

#### 2.4.3. Method A: Monte Carlo simulation (benchmark)

A robust reliability method is Crude Monte Carlo Simulation, which is illustrated in Figure 5(a). First, all random variables are sampled from their distributions. Time-invariant parameters  $X$  (levee properties and flood fighting interventions) are sampled only for the first year of the analysis, and remain constant throughout the analysis period. Time-variant parameters  $(h_p, D_p)$  are resampled each year from their distribution, assuming independence between years.  $N_t$  is the number of years in the analysis period. The initial (pre-storm) pipe length  $l_{ini}$  is 0 in the first year of the analysis. Pipe length development over the analysis period  $l_e(t)$  is calculated for each sample (denoted by index  $n$ ) separately using the pipe progression model described in Section 2.3 and the sampled variables  $h_p^n(t)$ ,  $D_p^n(t)$ , and  $X^n$ . Strength recovery between flood events is included by multiplying  $l_e$  with a factor  $(1 - r_l)$ , where  $0 < r_l < 1$  is a pipe length recovery fraction per year. Recovery occurs only when  $l_e < L$  (non-failure). In case of failure ( $l_e \geq L$ ), the levee is not repaired, thus failed samples stay failed for the rest of the analysis period. The failure probability in each year  $P_f(t)$  is obtained by counting the samples where  $l_e \geq L$  and dividing by the number of samples  $N_s$ :

$$P_f(t) = P(l_e(t) \geq L) = \frac{\sum_{n=1}^{N_s} \mathbf{I}(l_e^n(t) \geq L)}{N_s} \quad (14)$$

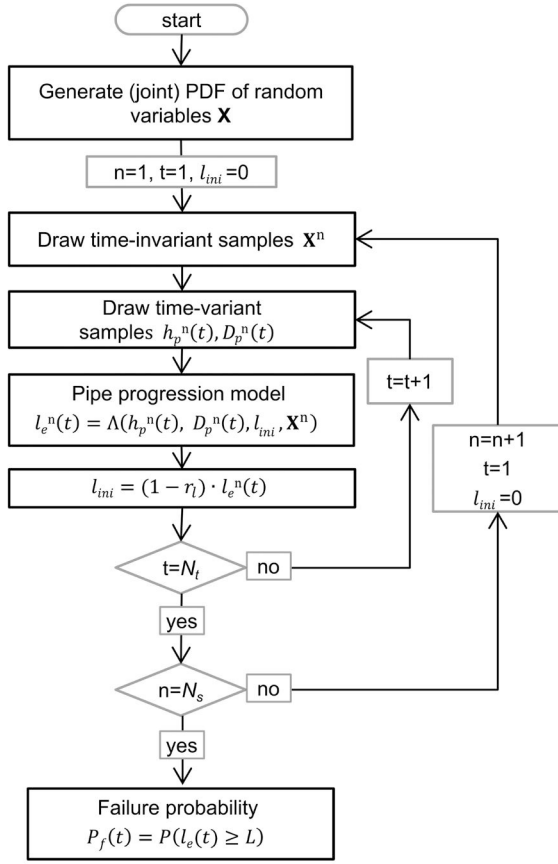
This gives the probability that the levee is in the failed state in year  $t$ ; hence it failed in the time interval  $[0, t]$ . The required number of model evaluations equals  $N_s \cdot N_t$ .

#### 2.4.4. Method B: Monte Carlo with numerical integration

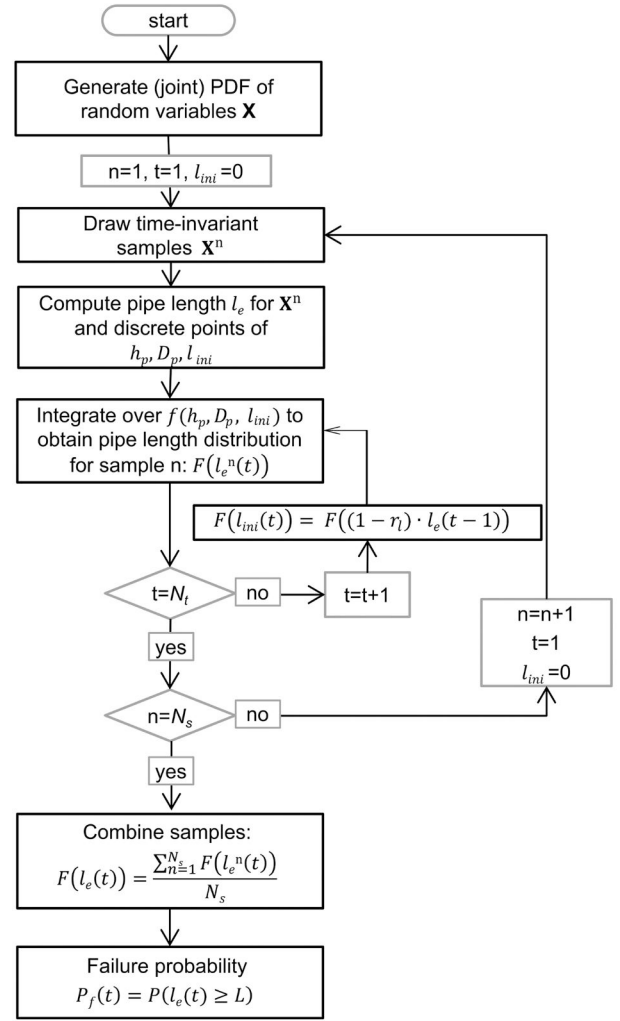
Method B separates extreme loads (for which we use numerical integration) from structural strength (for which we use Monte Carlo sampling). In Method B, the pipe development over the analysis period is also calculated for each Monte Carlo sample separately, using three sources of information: (1) the initial pipe length  $l_{ini}$ , (2) the (joint) distribution of hydraulic loads  $f(h_p, D_p)$ , and (3) the relation between the pipe length at the end of a flood event ( $l_e$ ) and the initial pipe length and hydraulic loads. However, in method B, the hydraulic loads are not sampled from their distributions, as in method A. Instead, the load variables are discretized and the pipe length development is calculated conditional on these discrete integration points and then integrated over the load distributions. This is similar to a fragility curve approach (Shinozuka, Feng, Lee, & Naganuma, 2000; van der Meer, ter Horst, & van Velzen, 2009) but extended to time-dependent reliability. Figure 5(b) shows the calculation procedure.

The cumulative probability distribution (CDF) of the pipe length  $l_e$  in a single MC sample  $n$  at the end of year  $t$  is given by:





(a) Method A: Crude Monte Carlo Simulation.



(b) Method B: Monte Carlo + Numerical Integration.

Figure 5. Flowcharts of probabilistic methods A (MC) and B (MC+NI).

$$F(l_e^n, t) = \int_{l_{ini}(t)} \int_{D_p} \int_{h_p} I(\Lambda(h_p, D_p, l_{ini}(t), \mathbf{X}^n) < l_e) \cdot f(h_p, D_p, l_{ini}(t)) dh_p dD_p dl_{ini} \quad (15)$$

Here,  $h_p$  denotes peak water level,  $l_{ini}$  the pipe length prior to an extreme event,  $D_p$  peak flood duration,  $\mathbf{X}^n$  the time-invariant levee properties of sample  $n$ . The indicator function  $I(\cdot)$  equals 1 if true and 0 otherwise. The function  $l_e = \Lambda(h_p, D_p, l_{ini}, \mathbf{X}^n)$  is the pipe progression model from Section 2.3.  $f(h_p, D_p, l_{ini})$  is the joint distribution (PDF) of hydraulic loads and  $l_{ini}$ . Here, these three variables are assumed independent and the joint PDF can be replaced by the product of marginal distributions:  $f(h_p)f(D_p)f(l_{ini})$

The initial pipe length distribution in the first year of the analysis,  $f(l_{ini}(0))$ , needs to be assumed or set to a fixed value. For each year in the analysis period, the distribution of  $l_e$  is updated with Equation (15). In the absence of strength recovery between flood events, the end pipe length distribution is taken to the next year:  $F(l_{ini}(t)) = F(l_e(t-1))$ . Strength recovery is included by shifting the pipe length

distribution so that  $F(l_{ini}(t)) = F((1 - r_l) \cdot l_e(t-1))$ , where  $0 < r_l < 1$  is the pipe length recovery fraction per year. The probability  $P(l_e \geq L)$  is not changed, as recovery cannot occur after failure. In this way, the pipe length distribution for each sample is updated each year. Equation (15) gives the numerical integration over the hydraulic loads and initial pipe length for a single MCS sample. Combination of all samples is done through:

$$F(l_e, t) = \frac{\sum_{n=1}^{N_s} F(l_e^n, t)}{N_s} \quad (16)$$

Now, the probability of being in the failed state  $P_f(t) = P(l_e(t) \geq L)$  is easily computed from Equation (16)

The required number of model evaluations in method B equals the product of  $N_s$  and the number of discrete evaluation points for  $h_p$  ( $N_h$ ),  $D_p$  ( $N_d$ ), and  $l_{ini}$  ( $N_l$ ). Unlike in method A, it does not depend on  $N_t$  and the exceedance probability of the extreme hydraulic loads. This is beneficial

Table 2. Distributions of random variables for the base case.

Parameter	Symb.	Unit	$\mu$	$\sigma$ , CoV	Distr.
Time-invariant:					
Seepage length	$L$	m	50	$\sigma=5$	Ln
Aquifer depth	$D_{aq}$	m	20	$\sigma=0.5$	Ln
Blanket thickness	$D_{bl}$	m	3	$\sigma=0.5$	Ln
Blanket weight	$\gamma_{sat,bl}$	kN/m <sup>3</sup>	18	$\sigma=1$	Ln
Critical heave gradient	$i_{c,h}$	–	0.7	$\sigma=0.1$	Ln
Grain size	$d_{70}$	mm	0.150	CoV = 0.1	Ln
Rolling angle	$\theta$	–	37	–	Det
White's coefficient	$\eta$	–	0.25	–	Det
Hydr. conductivity	$k_{aq}$	m/s	$1 \cdot 10^{-4}$	CoV = 0.5	Ln
Aquifer response	$r_e$	–	0.6	–	Det
Polder level	$h_e$	m + NAP	0	–	Det
Model factor uplift	$m_u$	–	1	$\sigma=0.1$	Ln
Model factor crit. head	$m_p$	–	1	$\sigma=0.12$	Ln
Pipe length at $t_0$	$l_0$	m	0	–	Det
Erosion coefficient	$C_e$	–	0.055	$\sigma=0.043$	Ln
Detection probability	$P_{ff}$	–	0.9	–	Det
Time flood fighting	$t_{ff}$	Hours	10	$\sigma=0.6$	Ln
Recovery rate	$r_l$	–/Year	0	–	Det
Time-varying:					
Peak water level	$h_p$	m + NAP		Gumbel(loc = 4, scale = 0.25)	
Peak duration (coast)	$D_p$	Hours	4	$\sigma=1$	Ln
Peak duration (river)	$D_p$	Hours	48	$\sigma=24$	Ln

$\mu$  : mean;  $\sigma$  : standard deviation; Ln: log-normal; det: deterministic.

when failure is governed by loads with a small exceedance probability, as shown with an example in Section 3.2.

### 3. Application to coastal and river levees

This section applies the methods from Section 2 to assess the influence of time-dependent pipe growth on the reliability of levees with short (coastal) and long-lasting (river) flood duration. First, a coastal base case illustrates several steps in the method (Sections 3.1 and 3.2). Then, Section 3.3 presents sensitivity analyses on this base case to investigate the influence of uncertainties which are hard to quantify, such as the effectiveness of flood fighting, a partially developed pipe being initially present and potential strength recovery between flood events. Finally, levee properties and hydraulic loads are systematically varied in Section 3.4 to investigate the contribution of time-dependent pipe growth under different levee conditions.

#### 3.1. Random variables in base case

Table 2 presents the distributions of random variables in the base case. Several levee variables are illustrated in Figure 1. The choice of random variables aims to yield realistic values for the strength and load variables of levees across The Netherlands that are susceptible to BEP. However, given the large variation in properties across levees encountered in the field, these values are only indicative. Section 3.4 analyzes the effect of time-dependent pipe growth for other levee properties. Distributions of  $i_{c,h}$ ,  $m_u$  and  $m_p$  are based on Schweckendiek et al. (2014). The distributions of the erosion coefficient  $C_e$  is based on calibration with multi-scale piping experiments (Pol, 2022). Random variables are described by a log-normal distribution, or deterministic. The  $\mu$  and  $\sigma$  in Table 2 are the mean and standard deviation of the variable, and are transformed to log-normal distribution parameters  $m$  and  $s$  using:

$$m = \ln \left( \mu^2 / \sqrt{\sigma^2 + \mu^2} \right), \quad s = \sqrt{\ln(\sigma^2 / \mu^2 + 1)} \quad (17)$$

Hydraulic loads in the base cases are chosen relatively high to obtain high failure probabilities (order of  $10^{-4}$  for time-dependent and  $10^{-1}$  for instantaneous pipe growth) to allow for a comparison with the Crude Monte Carlo method (A). The sensitivity analyses on the base case in Section 3.3 use method B, which allows for smaller (and more realistic) failure probabilities and hence lower hydraulic loads. The sample size  $N_s$  is chosen beforehand as  $10^4$  in the base case and sensitivity analyses, except for the coastal base case where  $N_s = 10^5$ . The number of discrete evaluation points for water level, duration and  $l_{ini}$  equal  $N_h=11$ ,  $N_d=3$ , and  $N_l=6$  in the base case. Both  $N_s$  and  $N_h$ ,  $N_d$  and  $N_l$  were chosen based on sensitivity calculations such that a further increase of these values would not result in significantly different failure probabilities.

The time-invariant levee properties in Table 2 are considered fully correlated in time, whereas peak water level and peak duration are considered uncorrelated in time. Some levee properties may be correlated due to physical relations (e.g. grain size with hydraulic conductivity), but these correlations between variables are neglected in this analysis. Spatial correlation is not considered, as this analysis is limited to single levee cross-sections. Cross-section results can be combined to a system level failure probability using the same methods as time-invariant analyses (Steenbergen, Lassing, Vrouwenvelder, & Waarts, 2004).

#### 3.1.1. Flood fighting interventions

Timely flood fighting interventions (emergency measures) may stop the erosion process and avoid failure because BEP is a relatively slow failure process which is observable by sand boils. Common interventions create counter-pressure

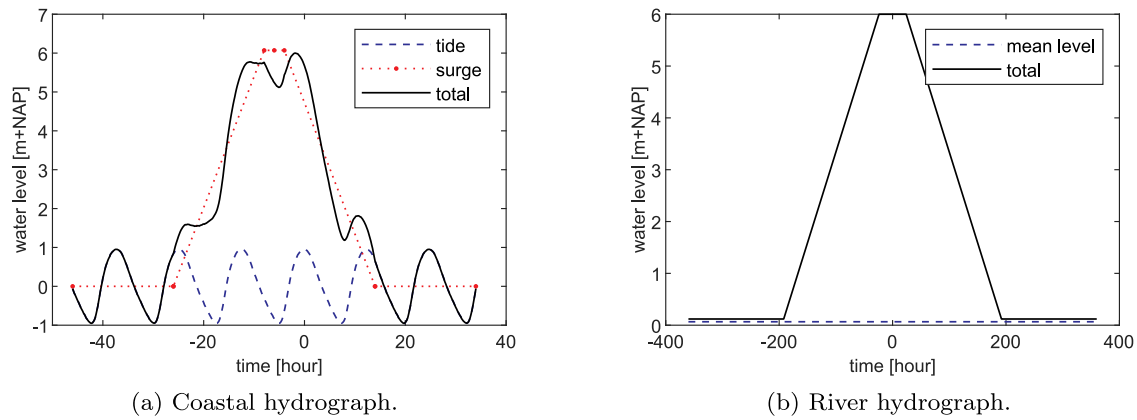


Figure 6. Modeling of coastal (a) and riverine (b) water level variation within extreme event as a trapezoidal water level setup. (a) Coastal hydrograph. (b) River hydrograph.

by locally raising the polder head (Nagy, 2014) or block the sand transport using filters (Montalvo-Bartolomei & Robbins, 2020). The likelihood of a timely, successful flood fighting intervention depends on factors such as detection error, placement error, structural failure and the required time for these actions (Barendregt, van Noortwijk, van der Doef, & Holterman, 2005; Jonkman, Dupuits, & Havinga, 2012; Lendering, Jonkman, & Kok, 2016). These depend in turn on organizational and logistical factors and will be site-specific. It is noted that the probability of a successful intervention will likely decrease with increasing water level, as both the number and severity of sand boils will increase but the organization's capacity is limited. To include all these aspects is beyond the scope of this study. For the base case, it is assumed that the probability of successful detection  $P_{ff}$  is 0.9 and the required time for successful flood fighting  $t_{ff}$  has a mean of 10 and standard deviation of 0.6 h. These estimates are based on experiences from flood fighting exercises (Jonkman et al., 2012; Lendering, Jonkman, & Kok, 2014; USBR & USACE, 2019; van Rinsum, 2018). It is noted that in coastal areas, extreme water levels occur during extreme storms in which detection and emergency operations may be more difficult.

### 3.1.2. Hydraulic load duration

The base case is analyzed with two extremes in terms of hydraulic load duration: a relatively short coastal storm surge and a long-lasting riverine flood. The method for modeling the water level variation within this annual maximum event depends on the source(s) of the extreme event (storm surge or river flood), as shown in Figure 6.

For levees loaded only by storm surge, the total water level is the sum of tidal variation and storm surge:  $h(t) = h_{tide}(t) + h_{surge}(t)$ . The tidal amplitude is 1 m and the tidal period 12 h in the base case. The storm surge is simply modeled as trapezoid with a peak duration  $D_p$  and a base duration  $D_0$ . The peak duration  $D_p$  has a mean value of 4 h and standard deviation of 1 h (Asselman, Peeters, & Coen, 2010; de Moel, Asselman, & Aerts, 2012). The base duration  $D_0$  is approximately ten times  $D_p$ . To avoid unrealistically short base durations in case of small values for  $D_p$ , it is assumed that  $D_0 = 20 + 5D_p$ . The assumed phase difference

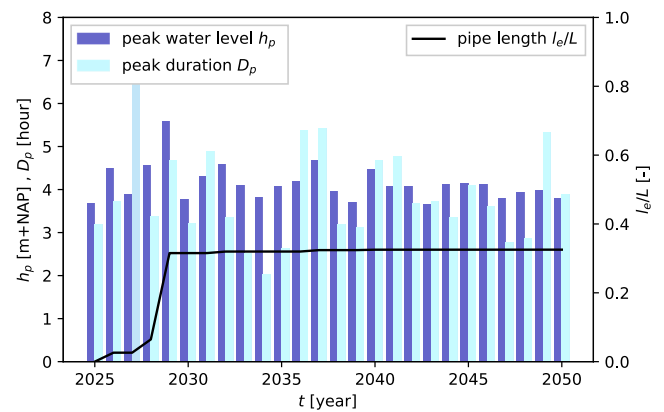


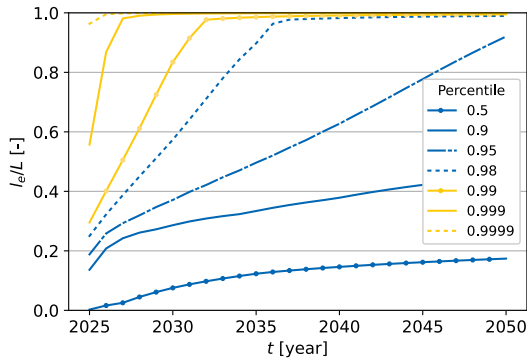
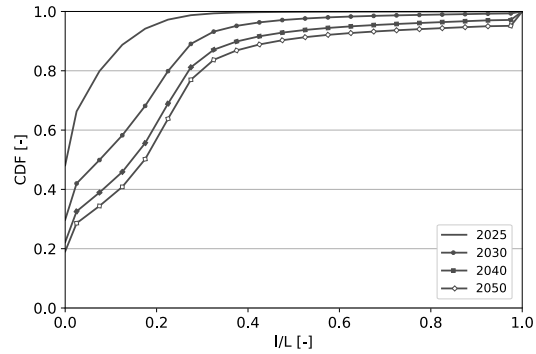
Figure 7. Pipe length development and yearly hydraulic loads for one sample of the coastal base case (method A).

between the peak of the storm surge and the maximum tide is 6 h, corresponding to half of the tidal period. This ensures that the surge peak aligns with low tide. In this way, the time-variation of the water level within an extreme event is described by two random variables:  $h_p$  and  $D_p$ . To obtain the time-varying water level for a given  $h_p$ , the normalized surge trapezium is scaled to the required peak level.

In case of levees loaded by high river discharges, the total water level is the sum of mean water level  $h_0$  and a trapezoid with a peak duration  $D_p$  and a base duration  $D_0$ . For the Rhine river, the peak duration  $D_p$  is assumed to have a mean value of 48 h and standard deviation of 24 h, and follows a log-normal distribution. The base duration  $D_0$  is taken as  $D_0 = 240 + 3D_p$  [hours].

### 3.2. Base case results

In this section, the coastal base case is used to illustrate typical steps of the reliability computation, and to compare the proposed MC+NI method (B) with the full Monte Carlo benchmark method (A). Figure 7 shows the deterministic pipe length development over time together with the annual maximum peak water levels and peak durations for one random Monte Carlo sample of the coastal base case. This is the same sample as illustrated in Figure 4. Uplift occurs when a critical water level of approximately 3.5 m + NAP is

(a) Percentiles of pipe length distribution  $l/L$ .

(b) CDF of pipe length in several years.

**Figure 8.** Pipe length development over the analysis period for the coastal base case. (a) Percentiles of pipe length distribution  $l/L$ . (b) CDF of pipe length in several years.

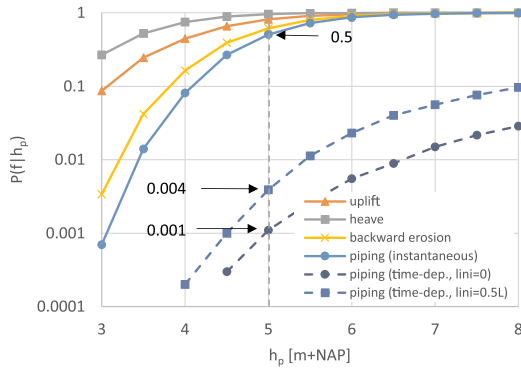


**Figure 9.** Conditional failure probabilities (fragility curves) for coastal base case with  $D_p=4$  h, and  $l_{ini}/L=0-0.5$ .

exceeded. This level is exceeded in most years and pipe growth starts early in the calculation period. A more extreme storm with a peak level around 5.5 m arrives in 2029, which increases the pipe length strongly to  $0.3L$ . In subsequent years, hardly any pipe growth occurs, even in years with a relatively high peak level of 4.5 m. This is because the equilibrium head  $H_{eq}$  for backward erosion is higher at pipe length  $l = 0.3L$  than at  $l = 0$  (Figure 3). In this sample, the critical head for BEP  $H_c$  is around 5 m and is not exceeded in the period up to 2050.

Although the pipe length might develop shock-wise within a single sample, the development averaged over all samples is gradual, as shown by the percentiles in Figure 8(a). This figure shows for instance that the failure probability in 2035 is approximately 2% (0.98 percentile line reaches  $l/L = 1$ ). Figure 8(b) shows the cumulative distribution (CDF) of the pipe length in several years, indicating that most pipe growth occurs in the first years of the calculation period due to a small number of relatively weak samples.

Failure probabilities conditional on the main hydraulic load (fragility curves) are an intuitive way to interpret reliability analysis results. Figure 9 shows the fragility curves of different components of the failure process, for the coastal base case. Given a hydraulic load of  $h_p = 5$  m and  $D_p = 4$  hours and initial pipe length  $l_{ini} = 0$ , the conditional piping failure probability without time-dependence (instantaneous pipe growth) equals 0.6. The resistance appears to be dominated by the critical head for BEP  $H_c$ , as uplift and heave

probabilities are close to 1. Including the time-dependent pipe growth reduces the failure probability  $P_f|_{h, D_p, l_{ini}}$  to 0.002. Apparently, it is highly unlikely that the pipe progresses under the entire levee in one such storm, despite the critical head for BEP  $H_c$  being exceeded. To assess the sensitivity of the model to pipes from previous flood events, a computation with  $l_{ini} = 0.5L$  is included. This increases the conditional failure probability to 0.004, which is still significantly lower than that of the instantaneous model.

After incorporating the probability distributions of the hydraulic loads with probabilistic methods A and B, the resulting (cumulative) failure probabilities for the coastal base case are shown in Figure 10. It appears that method B gives similar results compared to the benchmark method A. Remaining differences between the two methods decrease with a smaller step size in the numerical integration of the hydraulic loads. In the first analysis year (2025), the failure probability with instantaneous pipe growth equals 0.1 and with time-dependent pipe growth 0.0001; a factor of 1000 difference. This  $P_f(2025)$  represents the probability of complete pipe development from 0 to  $L$  within a single flood event. In subsequent years, the difference becomes smaller as the pipe length increases in the time-dependent case, resulting in approximately a factor of 10 difference by 2050. The trend in the conditional failure rate (Figure 10(b)) is a combination of two effects: an increasing  $\lambda$  over time due to increasing pipe length (degradation, which is only present in the time-dependent erosion case) and a decreasing  $\lambda$  as the strongest samples survive over time. In case of small failure probabilities,  $\lambda$  of the instantaneous case will be almost constant over time as the probability of survival approaches 1.

### 3.3. Sensitivity analysis on base case

This sensitivity analysis quantifies how the base case failure probabilities and the effect of time-dependence change when different assumptions are used regarding the safety level and three factors which are largely unknown in practice: effectiveness of flood fighting, a pipe being initially present due to previous erosion, and strength recovery between extreme events. Results are summarized in Table 3. The

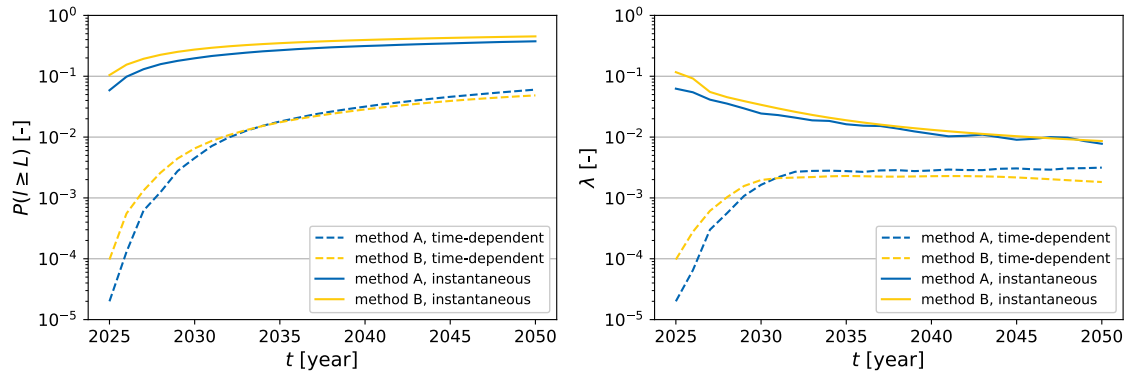
(a) Cumulative failure probability  $P(I \geq L)$ .(b) Conditional failure rate  $\lambda$ .

Figure 10. Cumulative and conditional failure rate over time for the coastal base case. Comparison of probabilistic methods A (MC) and B (MC+NI), with instantaneous pipe growth and time-dependent pipe growth according to Equation (5). (a) Cumulative failure probability  $P(I \geq L)$ . (b) Conditional failure rate  $\lambda$ .

Table 3. Results of the reliability analyses, including cases in sensitivity analysis

Case	2025			2050			
	$P_{f,td}$	$P_{f,stat}$	$F_{td}$	$P_{f,td}$	$P_{f,stat}$	$F_{td}$	
Base case – probabilistic method:							
1a	Base case – coast – A	$2.0 \cdot 10^{-5}$	$5.9 \cdot 10^{-2}$	2900	$6.0 \cdot 10^{-2}$	$3.8 \cdot 10^{-1}$	6.2
1b	Base case – coast – B	$9.7 \cdot 10^{-5}$	$1.0 \cdot 10^{-1}$	1100	$4.8 \cdot 10^{-2}$	$4.5 \cdot 10^{-1}$	9.3
1c	Base case – river – A	$2.7 \cdot 10^{-3}$	$4.5 \cdot 10^{-2}$	17	$6.9 \cdot 10^{-2}$	$2.7 \cdot 10^{-1}$	4.0
1d	Base case – river – B	$2.8 \cdot 10^{-3}$	$7.4 \cdot 10^{-2}$	26	$6.1 \cdot 10^{-2}$	$3.3 \cdot 10^{-1}$	5.4
Effect of higher safety level:							
2a	$h_p \sim \text{Gum}(3.5, 0.25)$ – coast – B	$1.4 \cdot 10^{-5}$	$2.9 \cdot 10^{-2}$	2100	$9.2 \cdot 10^{-3}$	$2.2 \cdot 10^{-1}$	24
2b	$h_p \sim \text{Gum}(3, 0.25)$ – coast – B	$1.9 \cdot 10^{-6}$	$5.6 \cdot 10^{-3}$	2900	$9.0 \cdot 10^{-4}$	$8.4 \cdot 10^{-2}$	94
2c	$h_p \sim \text{Gum}(3.5, 0.25)$ – river – B	$7.0 \cdot 10^{-4}$	$2.2 \cdot 10^{-2}$	32	$2.2 \cdot 10^{-2}$	$1.6 \cdot 10^{-1}$	7.3
2d	$h_p \sim \text{Gum}(3, 0.25)$ – river – B	$1.1 \cdot 10^{-4}$	$4.4 \cdot 10^{-3}$	38	$5.3 \cdot 10^{-3}$	$6.0 \cdot 10^{-2}$	11
Effect of flood fighting:							
all:	$h_p \sim \text{Gum}(3, 0.25)$ – method B						
3a	$t_{ff} = 24$ – coast	$9.0 \cdot 10^{-6}$	$6.8 \cdot 10^{-3}$	760	$2.5 \cdot 10^{-3}$	$9.8 \cdot 10^{-2}$	39
3b	$P_{ff} = 0$ – coast	$9.0 \cdot 10^{-6}$	$6.8 \cdot 10^{-3}$	760	$2.5 \cdot 10^{-3}$	$9.8 \cdot 10^{-2}$	39
3c	$t_{ff} = 24$ – river	$1.9 \cdot 10^{-4}$	$6.0 \cdot 10^{-3}$	31	$1.3 \cdot 10^{-2}$	$9.9 \cdot 10^{-2}$	7.7
3d	$P_{ff} = 0$ – river	$1.1 \cdot 10^{-3}$	$7.3 \cdot 10^{-3}$	6.5	$3.7 \cdot 10^{-2}$	$1.0 \cdot 10^{-1}$	2.8
Effect of an initial pipe:							
all:	$h_p \sim \text{Gum}(3, 0.25)$ – method B						
4a	$l_0 = 0.25L$ – coast	$2.0 \cdot 10^{-5}$	$5.6 \cdot 10^{-3}$	270	$1.5 \cdot 10^{-3}$	$8.4 \cdot 10^{-2}$	56
4b	$l_0 = 0.50L$ – coast	$2.1 \cdot 10^{-5}$	$5.6 \cdot 10^{-3}$	260	$2.2 \cdot 10^{-3}$	$8.4 \cdot 10^{-2}$	37
4c	$l_0 = 0.75L$ – coast	$1.0 \cdot 10^{-4}$	$5.6 \cdot 10^{-3}$	55	$5.4 \cdot 10^{-3}$	$8.4 \cdot 10^{-2}$	16
4d	$l_0 = 0.25L$ – river	$3.1 \cdot 10^{-4}$	$4.4 \cdot 10^{-3}$	14	$8.6 \cdot 10^{-3}$	$6.0 \cdot 10^{-2}$	7.0
4e	$l_0 = 0.50L$ – river	$3.2 \cdot 10^{-4}$	$4.4 \cdot 10^{-3}$	14	$1.1 \cdot 10^{-2}$	$6.0 \cdot 10^{-2}$	5.7
4f	$l_0 = 0.75L$ – river	$7.4 \cdot 10^{-4}$	$4.4 \cdot 10^{-3}$	6	$1.6 \cdot 10^{-2}$	$6.0 \cdot 10^{-2}$	3.7
Effect of recovery rate:							
all:	$h_p \sim \text{Gum}(3, 0.25)$ – method B						
5a	$r_l = 5\%/y$ – coast	$1.9 \cdot 10^{-6}$	$5.6 \cdot 10^{-3}$	2900	$3.4 \cdot 10^{-4}$	$8.4 \cdot 10^{-2}$	240
5b	$r_l = 10\%/y$ – coast	$1.9 \cdot 10^{-6}$	$5.6 \cdot 10^{-3}$	2900	$2.4 \cdot 10^{-4}$	$8.4 \cdot 10^{-2}$	350
5c	$r_l = 5\%/y$ – river	$1.1 \cdot 10^{-4}$	$4.4 \cdot 10^{-3}$	38	$3.4 \cdot 10^{-3}$	$6.0 \cdot 10^{-2}$	18
5d	$r_l = 10\%/y$ – river	$1.1 \cdot 10^{-4}$	$4.4 \cdot 10^{-3}$	38	$2.8 \cdot 10^{-3}$	$6.0 \cdot 10^{-2}$	22

$P_{f,td}$  denotes (cumulative) failure probability including time-dependence, and  $P_{f,stat}$  is without time-dependence (instantaneous). Effect of time-dependence is expressed by  $F_{td} = P_{f,stat}/P_{f,td}$ . A and B refer to the probabilistic methods.

discussion below focuses on the effect of time-dependent pipe growth on the reliability as expressed in  $F_{td}$  for the year 2050. This factor is defined as the ratio of cumulative failure probabilities with instantaneous ( $P_{f,stat}$ ) and time-dependent ( $P_{f,td}$ ) pipe growth:

$$F_{td} = \frac{P_{f,stat}}{P_{f,td}} \quad (18)$$

Effects of a higher safety level are investigated by lowering the peak water levels by 0.5 and 1 m, using a Gumbel location parameter of 3.5 and 3 m instead of 4 m in the base case. For both the coastal and river case, the difference

between time-dependent and instantaneous pipe growth increases with a higher safety level. As extreme events occur less frequently, cumulative growth of the pipe length takes more years, and the failure probability increases more slowly over time.

Effects of flood fighting are studied by two scenarios: (1) increasing the required time for successful flood fighting to  $t_{ff} \sim LN(\mu = 24, \sigma = 2)$  hours, and (2) by setting the probability of successful flood fighting  $P_{ff}$  to 0 (no flood fighting). The results in Table 3 indicate that flood fighting is an important factor in the failure probability for river levees, as it explains the majority of the difference in failure probability between time-dependent and instantaneous pipe growth

(compare case 3d and 1d). On the other hand, for coastal levees the effectiveness of flood fighting is of minor importance due to the relatively short flood duration. It has only an effect when the time required for interventions ( $t_{ff}$ ) is short. The case with  $t_{ff} \sim LN(\mu = 24, \sigma = 2)$  yields the same failure probability as the case without any flood fighting, as the storm has usually passed 24 h after the sand boiling started.

Effects of a potentially present pipe developed in previous extreme events are investigated by setting the initial pipe length in the first year equal to  $0.25$ ,  $0.50$  or  $0.75L$  instead of  $0L$ . The case with  $0.50L$  is already rather extreme because it implies that the critical head for backward erosion has been exceeded. For both the coastal and river case, the effect of an initial pipe length up to  $0.50L$  is limited. This can be explained from the shape of the equilibrium curve (Figure 3), which results in more rapid pipe growth in the initial regressive phase ( $l < l_c$ ). Therefore, most of the time required for erosion and hence the contribution to time-dependent reliability is associated with the progressive phase ( $l > l_c$ ).

In the probabilistic model, strength recovery between extreme events is represented by a decrease of the pipe length between two consecutive years. Sensitivity of the results for strength recovery are studied using recovery rates ( $r_l$ ) of 5 and 10%. The results in Table 3 indicate that strength recovery can affect the reliability on the long term. For instance, 10% pipe length recovery per year in the coastal base case results in a factor 4 difference in failure probability in 2050 (comparing case 2b and 5b). Strength recovery will have a relatively large effect when it takes multiple storms for the pipe to progress through the levee. This explains why the effect is smaller for the river case (case 2d and 5d) where failure relatively often develops within a single flood event due to the long flood duration.

As noted in Section 2.4, method A and B differ in the required number of model evaluations. Figure 11 illustrates this for the river and coastal base cases. It shows how the time-dependent failure probability ( $P_{f,td}$ ) in 2025 depends on the sample size  $N_s$ . It shows that the convergence of method B is slightly faster than in method A (river and coast). This can be explained from the fact that in method B, the uncertainty in  $h_p$  is solved by numerical integration

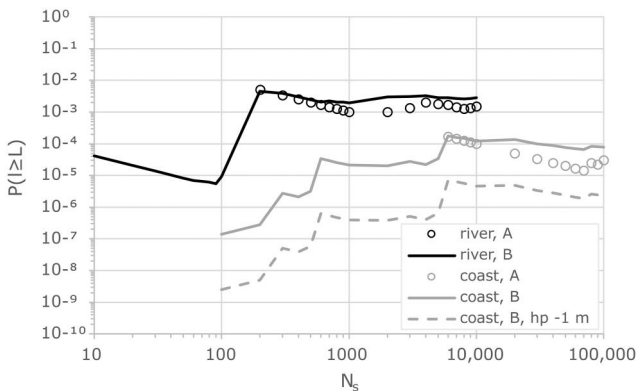


Figure 11. Convergence of failure probability  $P(l \geq L)$  with increasing sample size  $N_s$  for different cases with method A and B.

and not sampled. Considering that in this case  $N_t=25$ ,  $N_h=11$ ,  $N_d=3$ , and  $N_f=6$ , the number of evaluations with method B is larger than in method A. However, for the coastal base case with 1 m lower peak water levels and associated lower failure probability ('coast, B, 2025, hp -1 m'), the convergence remains the same. With the same number of model evaluations, a lower failure probability can be computed, which is not possible with Monte Carlo. Hence the combination of Monte Carlo for the strength and Numerical Integration for the loads is suitable for cases with small probabilities where failure is governed by extreme load events.

### 3.4. Influence of levee characteristics

To study the conditions under which time-dependent pipe growth significantly affects reliability, this section analyzes the influence of several factors, which are expected to be important for the time-dependent pipe growth. The first factor is the relation between the time required for pipe development (seepage length and progression rate) and the flood duration. This is taken into account by varying the seepage length  $L$ , grain size  $d_{70}$  (and associated hydraulic conductivity), and analyzing the extreme load scenarios of a short coastal storm surge and a long-lasting river flood. Second, the blanket thickness  $D_{bl}$  is varied to obtain different ratios of uplift resistance and backward erosion piping resistance. If the critical head for uplift is higher than the critical head for backward erosion, the erosion starts relatively late in the flood event, but once it occurs it will progress faster because it is more strongly overloaded. Thick blankets also result in a high resistance in the vertical pipe due to the  $0.3D_{bl}$ -reduction in Equation (6); in that way, the erosion process stops earlier when the flood level is falling.

The analyzed mean values of each variable are:

- $L$ : 50, 100 and 150 m
- $d_{70}$ : 200 and 400  $\mu\text{m}$
- $k_{aq}$ :  $1 \cdot 10^{-4}$  and  $4 \cdot 10^{-4}$  m/s (coupled to  $d_{70}$ )
- $D_{bl}$ : 1 and 5 m

The standard deviations or coefficients of variation are equal to the values in Table 2. The distribution of the peak water levels  $h_p$  is coupled to the seepage length. This results in wider levees being loaded with higher water levels to avoid large differences in instantaneous failure probability between cases with different seepage lengths. The Gumbel location parameters are 2.0 for  $L = 50$  m, 3.0 for  $L = 100$  m, and 4.0 for  $L = 150$  m. All analyses are without flood fighting and without strength recovery. Other variables are equal to those in Table 2. The sample size  $N_s = 10^4$ .

Results are expressed as factor  $F_{td}$  for the year 2050 (Equation (18)), which describes the effect of time-dependent pipe growth on the probability of failure until 2050. Figures 12 and 13 show the results for the different levee configurations. Differences in effect between coast and river due to differences in flood duration are clearly visible, as also shown in the base cases. The effect of time-dependent

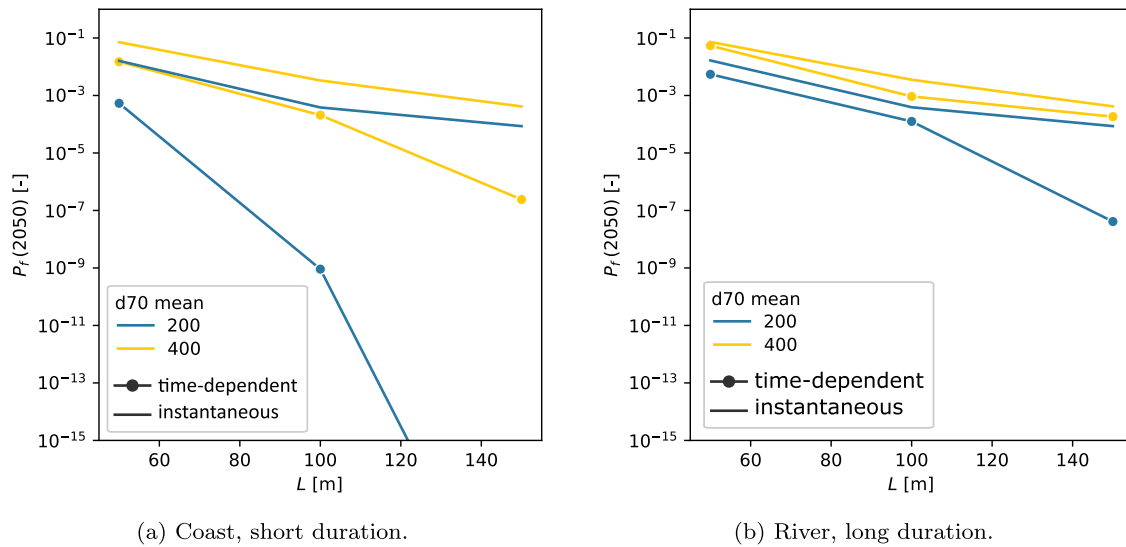


Figure 12. Probability of failure until 2050 ( $P_r(2050)$ ) with time-dependent and instantaneous pipe growth, as function of seepage length  $L$  [m] and grain size  $d_{70}$  [ $\mu$ m], for blanket thickness  $D_{bl} = 1$  m. Results for initially intact blanket and without flood fighting interventions. (a) Coast, short duration. (b) River, long duration.

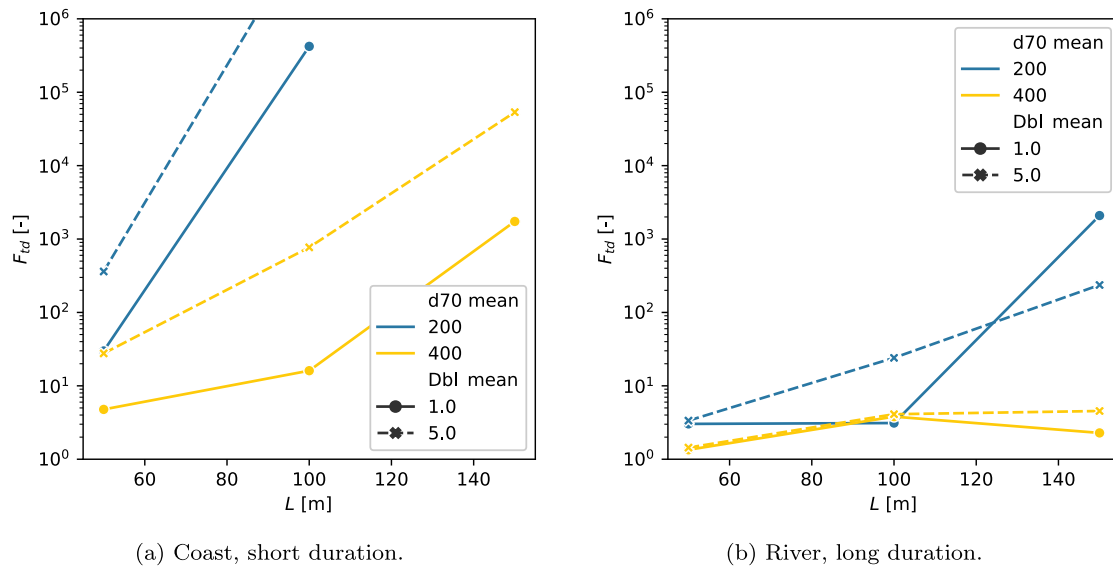


Figure 13. Effect of time-dependent pipe growth on reliability up to 2050 ( $F_{td}$ ) as function of seepage length  $L$  [m], grain size  $d_{70}$  [ $\mu$ m] and blanket thickness  $D_{bl}$  [m]. Results for initially intact blanket and without flood fighting interventions. (a) Coast, short duration. (b) River, long duration.

pipe growth is large in the coastal levee cases; it ranges from  $F_{td} \approx 5$  for coarse sand with a thin blanket and short seepage length up to  $F_{td} > 10^6$  for large seepage lengths and fine sand. Although effects are much smaller for the river levee cases, they can still be considerable (factor of 10–100) for particular situations such as fine sand combined with a large seepage length. In other situations with river levees (coarse sand and thin blanket) effects are limited ( $F_{td} < 5$ ) and the current assumption of instantaneous failure can be considered realistic.

### 3.5. Implications for levees in The Netherlands

The findings in this article have several implications for levee management in areas prone to piping failure. These areas are found near rivers and deltas around the world,

such as in China (Yangtze), France (Agly), Hungary (Danube), Italy (Po), Japan (Yabe), The Netherlands (Rhine-Meuse Delta), USA (Mississippi) and Vietnam (Red River Delta). This section focuses on the context of The Netherlands with respect to (1) extension of results to other types of water systems and (2) discussing a simplified decision rule in current levee guidelines.

Results in Figure 13 show large differences in the effect of time-dependent pipe growth ( $F_{td}$ ) between the two extreme cases in terms of the hydraulic load duration: coastal storm surge and Rhine river floods. Delta regions subject to both storm surge and river discharge will fall somewhere in between these extremes. Examples of areas with such compound events are the Rhine-Meuse Delta and IJssel-Vecht Delta in the Netherlands (see box in Figure 14). Extreme events in these delta's are composed a long base

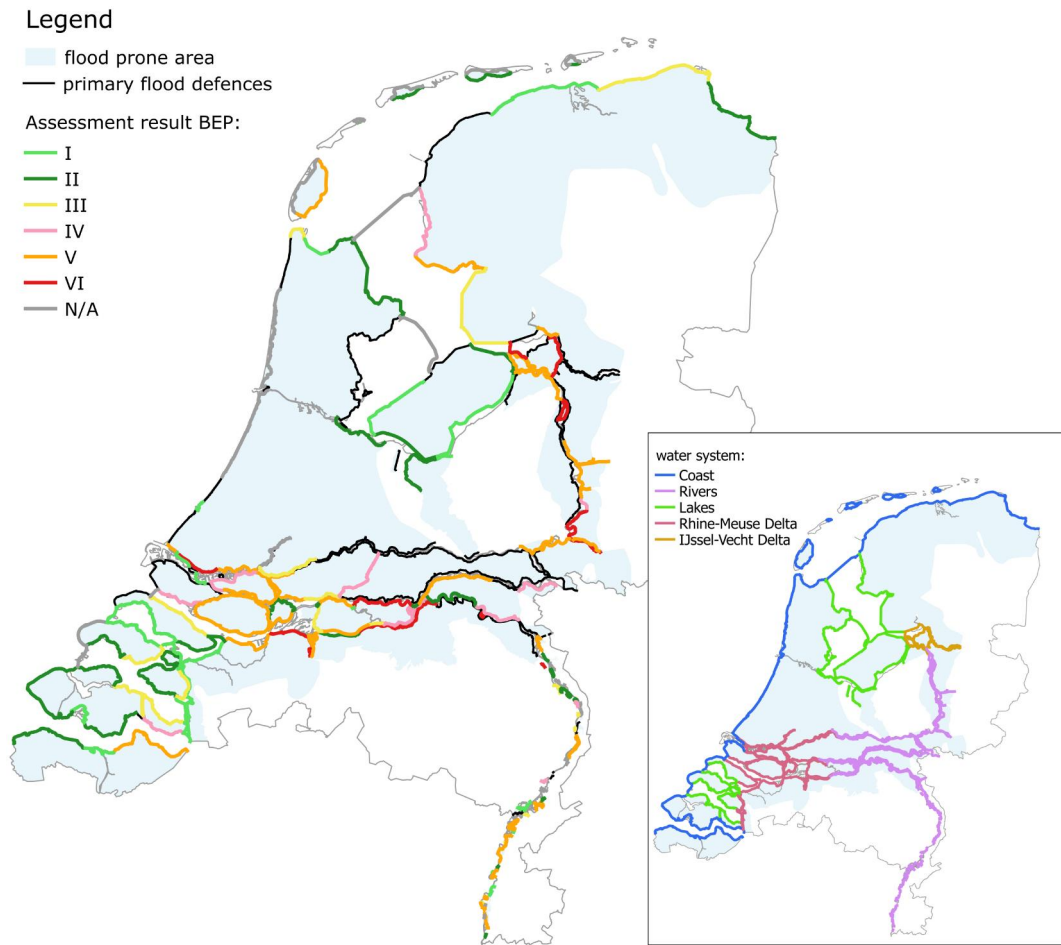


**Figure 14.** National safety assessment results for backward erosion piping in levees. *Data source:* Dutch National Georegister (Georegister, 2021). Categories indicate distance between computed safety level and local safety standard. Categories I–III comply to the standards, categories V and VI do not comply, category IV is close to the standard.

duration from river floods and a short peak from storm surge. The methods in this article also apply to these areas with compound flood events, but with multiple load variables which may be correlated. Furthermore, floods in the Meuse river are on average shorter compared to the Rhine river. To assess the potential of including time-dependent pipe development in safety assessment and design, this picture of water systems must be combined with the current safety assessment results for the piping failure mechanism (Figure 14). These assessment results are an indicator for future levee reinforcement projects. The map shows that a substantial number of levee segments along the coast, lakes and delta areas do not comply with the safety standards for piping (category V and VI) using piping models based on instantaneous erosion. These levees are expected to have a much higher reliability due to the limited time available for erosion.

Several real levee cases along the Dutch coast and tidal rivers have been analyzed using the time-dependent BEP model. One example is a tidal river levee with dimensions  $L \approx 50$  m,  $D \approx 15$  m, and grain size  $d_{70} \approx 0.200$  mm. During the highest observed head drop in 40 years (3.5 m), no sand boils were observed here. A stationary BEP analysis yielded a conditional failure probability in the order of 10%

for this event; relatively high given the absence of sand boils. In contrast, employing a time-dependent BEP analysis resulted in a conditional failure probability on the order of  $10^{-4}$ , which better explains the observations.

Currently, the assessment guidelines for levees in the Netherlands contain a criterion for time-dependent pipe growth (Ministry of Infrastructure & Water Management, 2019). It states that the BEP failure probability is negligible when all of the following conditions are met:

- seepage length  $L > 50$  m;
- hydraulic loads are fully governed by storm surge (coast);
- it can be demonstrated that no sand boils have been observed in the past;
- emergency response plans include flood fighting interventions for the occurrence of two successive extreme flood events;
- there is no structure or crossing pipeline present in the levee.

The seepage length criterion is based on an average progression rate of 2 mm/s, which was considered an upper bound based on experiments, combined with a high water



level duration of 6 h (Jongejan & Van Beek, 2015). Thus, it accounts for the likelihood of full pipe growth within a single storm event while neglecting the resistance from uplift, heave, or critical head. With the methods presented in this article, the effects of time dependence can be expressed in terms of failure probability. Furthermore, these methods can be applied to situations where these conditions are not met, except for levees with structures and pipelines. For instance, the current limitation of this rule to coastal levees can be extended to include levees along lakes or delta systems. If emergency response plans are in place, their effectiveness can be quantified. Conversely, long-term cumulative pipe development can be assessed under the assumption of no emergency measures. Additionally, the current requirement that no sand boils have occurred can be replaced with an estimate of the initial pipe length that is currently present. Since simplified rules are valuable for practical application, the presented method can also be used to derive a similar set of criteria for 'safe' levees that is more broadly applicable, less conservative, and grounded in a stronger physical basis.

#### 4. Conclusions

The development of backward erosion piping (BEP) failure in flood defenses is subject to time constraints imposed by limitations in sand transport from the levee foundation. When the flood level falls before the pipe has developed in a hydraulic shortcut, or when timely flood fighting interventions are taken, the erosion process stops, preventing levee failure. This article introduces a method to quantitatively assess how this time-dependent factor influences the probability of levee failure.

First, a novel time-dependent piping failure model is formulated that is capable of including pipe growth in reliability analyses. It captures the relevant processes (uplift, heave, backward erosion, flood fighting) in a time-dependent and integrated manner. The rate of pipe development is calculated using a simplified formula derived from numerical simulations and experiments. Flood fighting, such as sand-bagging, is included through a probability of successful intervention and the time required for such an intervention. Subsequently, this model is incorporated into a time-variant reliability analysis framework using a combination of Monte Carlo Simulation and Numerical Integration to evaluate the influence of time dependence on levee reliability. Besides computing the current annual failure probability, the method shows how the reliability evolves over the years due to cumulative pipe growth over multiple flood events and potential strength recovery between these extreme events.

The effect of time-dependent pipe growth is quantified by the ratio of failure probability with and without time-dependent pipe growth ( $F_{td}$ ). Sensitivity analyses were conducted to show the influence of several factors on  $F_{td}$ . As expected, flood duration appears as an important factor: short coastal storm surges result in a higher  $F_{td}$  compared to longer river floods. For Dutch coastal levees, it is unlikely that a piping breach will develop within the duration of a

single extreme event. Conversely, Rhine river levees without flood fighting are likely to fail within a single event. The results indicate that a higher safety level yields a larger  $F_{td}$ . Flood fighting significantly contributes to the safety of river levees. In the coastal cases, flood fighting is only effective when the intervention time is short compared to the storm surge duration. The analysis showed that a previously formed short pipe does not have a significant impact on reliability. Recovery of pipes between flood events influences the long-term development of the failure probability, but reliable quantification of this recovery is currently not possible due to a lack of empirical evidence. As a conservative assumption, the effects of time-dependence can still be analyzed assuming no recovery.

A parametric study incorporating various levee characteristics and hydraulic loads indicated under which conditions a large effect of time-dependence ( $F_{td}$ ) may be expected. Influential levee properties are the seepage length and grain size (or permeability). Effects are large for coastal levees, ranging from  $F_{td} \approx 5$  up to more than  $10^6$ . Although effects are smaller in the river cases, they can still be considerable (factor 10–100) for particular situations, such as fine sand combined with a large seepage length. For other river cases involving coarse sand and very thin blankets, effects are limited ( $F_{td} < 5$ ) and the current assumption of instantaneous failure is considered realistic. Levees along the tidal rivers and deltas fall between these extremes, and are also expected to have a lower failure probability due to time-dependent pipe development.

Recommendations for further research include the use of more efficient probabilistic methods that still capture the dependence in strength between different years. It is also recommended to further validate the prediction model for the progression rate and underlying processes, in particular on larger scales. Finally, the variability in storm surge duration and its representation by a simplified hydrograph needs further study, as well as efficient methods for combined loads from storm surge and river discharge. Based on the results, it is concluded that, depending on the local conditions, considering time-dependent development of backward erosion piping can be crucial for a realistic reliability estimate of flood defenses. However, this approach is currently not implemented in practice. This article provides a method for conducting such quantitative probabilistic analyses.

#### Disclosure statement

No potential conflict of interest was reported by the author(s).

#### Funding

This work was supported by the Netherlands Organisation for Scientific Research (NWO) under [Grant P15-21D].

#### References

- Allan, R. (2018). *Backward erosion piping* (Doctoral dissertation). Sydney: University of New South Wales.

- Asselman, N. E. M., Peeters, P., & Coen, L. (2010). *LTV-OM thema Veiligheid, deelrapport 2: Analyse verloop van de maatgevende waterstand en bresgroei* (Report No. 1202019-000). Delft: Deltares.
- Baecher, G. B., & Christian, J. T. (2005). *Reliability and statistics in geotechnical engineering*. Chichester: John Wiley Sons.
- Barendregt, A., van Noortwijk, J., van der Doef, M., & Holterman, S. (2005, 23–25 May). Determining the time available for evacuation of a dike-ring area by expert judgement. In J. K. Vrijling, E. Ruijgh, & B. Stalenberg (Eds.), *Proceedings of the 9th International Symposium on Stochastic Hydraulics (ISSH)*, Nijmegen, The Netherlands: IAHR.
- Bligh, W. G. (1910). Dams, barrages and weirs on porous foundations. *Engineering News*, 64(26), 708–710.
- Buijs, F. A., Hall, J. W., Sayers, P. B., & Van Gelder, P. H. A. J. M. (2009). Time-dependent reliability analysis of flood defences. *Reliability Engineering & System Safety*, 94(12), 1942–1953. doi:10.1016/j.res.2009.06.012
- Calle, E. O. F., Dillingh, D., Meermaans, W., Vrouwenvelder, A. W. C. M., Vrijling, J. K., De Quellerij, L., & Wubs, A. J. (1985). Probabilistisch ontwerpen van waterkeringen (Report No. 18386). Delft: Rijkswaterstaat. <https://resolver.tudelft.nl/uuid:55ebf500-3c90-4f9c-bf64-261ccfe3244>
- Chen, H.-P., & Mehrabani, M. B. (2019). Reliability analysis and optimum maintenance of coastal flood defences using probabilistic deterioration modelling. *Reliability Engineering & System Safety*, 185, 163–174. doi:10.1016/j.res.2018.12.021
- Danka, J., & Zhang, L. (2015). Dike failure mechanisms and breaching parameters. *Journal of Geotechnical and Geoenvironmental Engineering*, 141(9), 04015039. doi:10.1061/(ASCE)GT.1943-5606.0001335
- de Moel, H., Asselman, N. E. M., & Aerts, J. C. J. H. (2012). Uncertainty and sensitivity analysis of coastal flood damage estimates in the west of the Netherlands. *Natural Hazards and Earth System Sciences*, 12(4), 1045–1058. doi:10.5194/nhess-12-1045-2012
- Foster, M., Fell, R., & Spannagle, M. (2000). The statistics of embankment dam failures and accidents. *Canadian Geotechnical Journal*, 37(5), 1000–1024. doi:10.1139/t00-030
- Georegister. (2021). Toets- en veiligheidsoordelen primaire waterkeringen (WBI) (Record No. bf447383-f2ae-47b0-b124-6c4db12ce689) [Data set]. Informatiehuis Water. <https://www.nationaalgeoregister.nl/>
- Hasofer, A. M., & Lind, N. C. (1974). Exact and invariant second-moment code format. *Journal of the Engineering Mechanics Division*, 100(1), 111–121. doi:10.1061/JMCEA3.0001848
- ICOLD. (2017). *Bulletin 164. Internal erosion of existing dams, levees and dikes, and their foundations*. France: ICOLD-CIGB.
- JCSS. (2001). Probabilistic model code – part 1 – basis of design. Joint Committee on Structural Safety. Retrieved from <https://www.jcss-ic.org/jcss-probabilistic-model-code/>.
- Jongejan, R., & Van Beek, V. M. (2015). Voorstel voor eenvoudige toetsregel o.b.v. tijd tot falen. Discussienotitie Voor WTI2017. Unpublished manuscript.
- Jonkman, S. N. (2005). Global perspectives on loss of human life caused by floods. *Natural Hazards*, 34(2), 151–175. doi:10.1007/s11069-004-8891-3
- Jonkman, S. N., Dupuits, E. J. C., & Havinga, F. (2012). The effects of flood fighting and emergency measures on the reliability of flood defences. In F. Klijn & T. Schweckendiek (Eds.), *Comprehensive flood risk management, Proceedings of flood risk: The 2nd European conference on flood risk management* (pp. 1–7). Boca Raton, FL: CRC Press.
- Jonkman, S. N., Voortman, H. G., Klerk, W. J., & van Vuren, S. (2018). Developments in the management of flood defences and hydraulic infrastructure in the Netherlands. *Structure and Infrastructure Engineering*, 14(7), 895–910. doi:10.1080/15732479.2018.1441317
- Kézdi, A. (1979). *Soil physics: Selected topics* (Vol. 25). Amsterdam: Elsevier.
- Kiureghian, A. D., & Ditlevsen, O. (2009). Aleatory or epistemic? Does it matter? *Structural Safety*, 31(2), 105–112. doi:10.1016/j.strusafe.2008.06.020
- Lendering, K. T., Jonkman, S. N., & Kok, M. (2014). Effectiveness and reliability of emergency measures for flood prevention. TU Delft & STOWA. Retrieved from: <http://resolver.tudelft.nl/uuid:72b2ab5d-a99b-4abc-9c27-d9ad69341217>.
- Lendering, K. T., Jonkman, S. N., & Kok, M. (2016). Effectiveness of emergency measures for flood prevention. *Journal of Flood Risk Management*, 9(4), 320–334. doi:10.1111/jjfr.12185
- Melchers, R. E., & Beck, A. T. (2017). *Structural reliability analysis and prediction*. Chichester, UK: John Wiley Sons Ltd.
- Ministry of Infrastructure and Water Management. (2019). Regeling veiligheid primaire waterkeringen 2017. Bijlage III Sterkte en veiligheid. Ministry of Infrastructure and Water Management. Retrieved from <https://iplo.nl/@205740/regeling-veiligheid-primaire-waterkeringen-2017/>.
- Montalvo-Bartolomei, A., & Robbins, B. (2020). Laboratory evaluation of lightweight sand boil filters. In *Proceedings of ASDSO Dam Safety 2019*. Orlando, Florida. Lexington: Association of State Dam Safety Officials.
- Nagy, L. (2014). *Buzgárok az árvízvédelemben*. Budapest: OVF Országos Vízügyi Főigazgatóság.
- Özer, I. E., van Damme, M., & Jonkman, S. N. (2019). Towards an International Levee Performance Database (ILPD) and its use for macro-scale analysis of levee breaches and failures. *Water*, 12(1), 119. doi:10.3390/w12010119
- Paté-Cornell, M. E. (1996). Uncertainties in risk analysis: Six levels of treatment. *Reliability Engineering & System Safety*, 54(2–3), 95–111. doi:10.1016/S0951-8320(96)00067-1
- Pol, J. C. (2022). *Time-dependent development of Backward Erosion Piping* (Doctoral dissertation). Delft: Delft University of Technology.
- Pol, J. C., Kanning, W., van Beek, V. M., Robbins, B. A., & Jonkman, S. N. (2022). Temporal evolution of backward erosion piping in small-scale experiments. *Acta Geotechnica*, 17(10), 4555–4576. doi:10.1007/s11440-022-01545-1
- Pol, J. C., Noordam, A., & Kanning, W. (2024). A 3D time-dependent backward erosion piping model. *Computers and Geotechnics*, 167, 106068. doi:10.1016/j.compgeo.2024.106068
- Rice, J., van Beek, V., & Bezuijen, A. (2021). History and future of backward erosion research. In J. Rice, X. Liu, I. Sasanakul, M. McIlroy, & M. Xiao (Eds.), 10th International Conference on Scour and Erosion (ICSE-10), Proceedings (pp. 1–23). American Society of Civil Engineers (ASCE).
- Rice, J. D., & Polanco, L. (2012). Reliability-based underseepage analysis in levees using a response surface–Monte Carlo simulation method. *Journal of Geotechnical and Geoenvironmental Engineering*, 138(7), 821–830. doi:10.1061/(ASCE)GT.1943-5606.0000650
- Riha, J., & Petruła, L. (2023). Experimental research on backward erosion piping progression. *Water*, 15(15), 2749. doi:10.3390/w15152749
- Robbins, B. A., van Beek, V. M., López-Soto, J. F., Montalvo-Bartolomei, A. M., & Murphy, J. (2018). A novel laboratory test for backward erosion piping. *International Journal of Physical Modelling in Geotechnics*, 18(5), 266–279. doi:10.1680/jphmg.17.00016
- Rosenbrand, E., Wopereis, L., Wiersma, A., Kanning, W., Bezuijen, A., & Blinde, J. (2022). *Kennis voor Keringen 2021: Achtergrondrapport Voorlanden*. Delft: Deltares.
- Rotunno, A. F., Callari, C., & Froiio, F. (2019). A finite element method for localized erosion in porous media with applications to backward piping in levees. *International Journal for Numerical and Analytical Methods in Geomechanics*, 43(1), 293–316. doi:10.1002/nag.2864
- Rubinstein, R. Y., & Kroese, D. P. (2008). *Simulation and the Monte Carlo method*. Chichester, UK: John Wiley Sons.
- Schweckendiek, T., Vrouwenvelder, A. C. W. M., & Calle, E. O. F. (2014). Updating piping reliability with field performance observations. *Structural Safety*, 47, 13–23. doi:10.1016/j.strusafe.2013.10.002
- Sellmeijer, J. B. (1988). *On the mechanism of piping under impervious structures* (Doctoral dissertation). Delft: Delft University of Technology.

- Sellmeijer, J. B. (2006). Numerical computation of seepage erosion below dams (piping). In H. J. Verheij & G. J. Hoffmans (Eds.), *Proceedings of the 3rd International Conference on Scour and Erosion (ICSE-3)* (pp. 596–601). Gouda: CURNET.
- Sellmeijer, H., de la Cruz, J. L., van Beek, V. M., & Knoeff, H. (2011). Fine-tuning of the backward erosion piping model through small-scale, medium-scale and IJkdijk experiments. *European Journal of Environmental and Civil Engineering*, 15(8), 1139–1154. doi:10.1080/19648189.2011.9714845
- Shinozuka, M., Feng, M. Q., Lee, J., & Naganuma, T. (2000). Statistical analysis of fragility curves. *Journal of Engineering Mechanics*, 126(12), 1224–1231. doi:10.1061/(ASCE)0733-9399(2000)126:12(1224)
- Slijkhuis, K. A. H., Van Gelder, P. H. A. J. M., Vrijling, J. K., & Vrouwenvelder, A. C. W. M. (1999). On the lack of information in hydraulic engineering models. In G. I. Schuëller & P. Kafka (Eds.), *Proceedings of ESREL99 – The Tenth European Conference on Safety and Reliability* (pp. 713–718). Rotterdam: Balkema.
- Steenbergen, H. M. G. M., Lassing, B., Vrouwenvelder, A. C. W. M., & Waarts, P. H. (2004). Reliability analysis of flood defence systems. *Heron*, 49(1), 51–73.
- TAW. (1999). Technical report on sand boils (piping) (Tech. Rep. No. TAW99-26). Rijkswaterstaat.
- USBR & USACE. (2019). Best practices in dam and levee safety risk analysis. <https://www.usbr.gov/ssle/damsafety/risk/methodology.html>.
- van Beek, V. M. (2015). *Backward erosion piping: Initiation and progression* (Doctoral dissertation). Delft: Delft University of Technology.
- Vandenboer, K., Celette, F., & Bezuijen, A. (2019). The effect of sudden critical and supercritical hydraulic loads on backward erosion piping: Small-scale experiments. *Acta Geotechnica*, 14(3), 783–794. doi:10.1007/s11440-018-0756-0
- van der Meer, J. W., ter Horst, W. L. A., & van Velzen, E. H. (2009). Calculation of fragility curves for flood defence assets. In P. Samuels, S. Huntington, W. Allsop, & J. Harrop (Eds.), *Flood risk management: Research and practice* (pp. 567–573). London: Taylor & Francis.
- van Rinsum, G. (2018). *Grass revetment reinforcements: A study into the effectiveness of measures applied during critical conditions* (Master's thesis). Delft: Delft University of Technology.
- Vorogushyn, S., Merz, B., & Apel, H. (2009). Development of dike fragility curves for piping and micro-instability breach mechanisms. *Natural Hazards and Earth System Sciences*, 9(4), 1383–1401. doi:10.5194/nhess-9-1383-2009
- Vrijling, J. K. (2001). Probabilistic design of water defense systems in The Netherlands. *Reliability Engineering & System Safety*, 74(3), 337–344. doi:10.1016/S0951-8320(01)00082-5
- Weijers, J. B. A., & Sellmeijer, J. B. (1993). A new model to deal with the piping mechanism. In J. Brauns, M. Herbaum, & U. Schuler (Eds.), *Proceedings of the International Conference Geo-filters* (pp. 349–355). Rotterdam: Balkema.
- Wesselink, A., Warner, J., Syed, M. A., Chan, F., Tran, D. D., Huq, H., ... Van Staveren, M. (2016). Trends in flood risk management in deltas around the world: Are we going soft? *International Journal of Water Governance*, 3(4), 25–46. doi:10.7564/15-IJWG90
- Wewer, M., Aguilar-López, J. P., Kok, M., & Bogaard, T. (2021). A transient backward erosion piping model based on laminar flow transport equations. *Computers and Geotechnics*, 132, 103992. doi:10.1016/j.compgeo.2020.103992
- Wolff, T. F. (2008). Reliability of levee systems. In K. K. Phoon (Ed.), *Reliability-based design in geotechnical engineering* (pp. 448–496). London: Taylor & Francis.